

SPARCML: High-Performance Sparse Communication for Machine Learning

Cédric Renggli
ETH Zurich

Dan Alistarh
IST Austria

Torsten Hoefler
ETH Zurich

Mehdi Aghagolzadeh
Microsoft

Abstract

One of the main drivers behind the rapid recent advances in machine learning has been the availability of efficient system support. Despite existing progress, scaling compute-intensive machine learning workloads to a large number of compute nodes is still a challenging task. In this paper, we address this challenge, by proposing SPARCML,¹ a general, scalable communication layer for machine learning applications. SPARCML is built on the observation that many distributed machine learning algorithms either have naturally sparse communication patterns, or have updates which can be sparsified in a structured way for improved performance, without loss of convergence or accuracy. To exploit this insight, we analyze, design, and implement a set of communication-efficient protocols for sparse input data, in conjunction with efficient machine learning algorithms which can leverage these primitives. Our communication protocols generalize standard collective operations, by allowing processes to contribute sparse input data vectors, of *heterogeneous sizes*. Our generic communication layer is enriched with additional features, such as support for non-blocking (asynchronous) operations and support for low-precision data representations. We validate our algorithmic results experimentally on a range of large-scale machine learning applications and target architectures, showing that we can leverage sparsity for order-of-magnitude runtime savings, compared to existing methods and frameworks.

1 Introduction and Motivation

A key enabling factor behind the recent progress in machine learning has been *efficient system support*, in the form of efficient hardware, e.g. [27], but also via specialized *software platforms*, e.g. [1, 10, 53]. Due to the sheer size of the datasets and models, production-scale machine learning workloads are usually *distributed* across multiple computing nodes, such as clusters of CPUs or GPUs in a datacenter environment. The arguably standard distribution strategy in machine learning is *data parallelism*, in which nodes partition the dataset, and maintain consistent copies of the set of model parameters by exchanging messages, either all-to-all, or through a coordinator node, called a parameter server [32]. The high *bandwidth* and *latency* requirements of these workloads put pressure on system scalability. For example, when training a deep neural network such as AlexNet [30] through stochastic gradient descent (SGD), nodes perform *all-to-all* exchanges of their gradient updates upon every batch of examples: the message size per node is > 200 MB, exchanged every few milliseconds. This communication can easily become the system bottleneck.

Given the significant impact of communication, significant effort has been invested into identifying scalable solutions. Virtually all major frameworks optimize for efficient communication [1, 10, 28, 42, 53], while

¹Stands for Sparse Communication layer for Machine Learning, to be read as *sparse ML*.

GPU vendors are developing specific communication layers for this goal [37]. The research community proposed several communication-reduction techniques, such as *quantization* [3,42], *asynchronous communication* [54], *structured sparsification* [2,13,44], or *large batch methods* [15,52]. However, scaling machine learning applications remains a complex process, requiring non-trivial insights.

Conceptual Contribution. We propose SPARCML, a scalable, general communication layer for machine learning. SPARCML starts from the idea that, to reduce communication and synchronization cost, we can exploit the *relaxed consistency* supported by machine learning applications. In particular, individual nodes can compute with an *inconsistent* view of the set of model parameters, which can be corrupted with noise from various sources, such as communication quantization or asynchrony. The immediate system implication, which we exploit in SPARCML, is that the updates which nodes wish to communicate are either *naturally sparse* [49], or can be *sparsified in a principled manner*, without loss of convergence [2, 3, 13,44].

Technical Contribution. Our thesis is that *exploiting sparsity and compression* should be standard when scaling machine learning applications. Surprisingly, support for efficient sparse communication or compression is currently neither available in standard communication libraries such as MPI [14], nor in specialized machine-learning communication libraries [37]. One possible reason is the fact that designing and implementing general sparse collective operations is non-trivial, as sparsity adds a new dimension to the already complex system trade-offs arising when implementing collective operations efficiently at scale [46].

We take on this challenge in SPARCML. Our implementation is efficient both in theory and in practice: for some workload parameters, it can be shown to be within constant factors of optimal in terms of bandwidth and latency cost. At the same time, our implementation achieves order-of-magnitude speedups versus highly optimized *dense collective* implementations, or over naive sparse implementations, both in synthetic tests and in real application scenarios. SPARCML has several additional features, such as efficient support for *reduced-precision collectives* and for *non-blocking* operations. For example, we can perform all-to-all sparse reductions for gradient exchange at 4 bits of precision per coordinate, overlapping computation and communication.

Targets. Our main target applications are two large-scale distributed machine learning tasks: training of state-of-the-art deep neural networks and large-scale regularized regression tasks. Our target systems are multi-node computing clusters. We study two scenarios: the first is *supercomputing*, where nodes are connected by a high-powered, extremely well optimized network. The second scenario is *datacenters*, where the network is *relatively* slower, such as InfiniBand or Gigabit Ethernet.

Challenges. The main algorithmic contribution behind our layer is a set of techniques for implementing collective communication operations, such as all-reduce sum, over a large number of nodes having input vectors that are *sparse*. The principal difficulty for designing and analyzing such algorithms lies in the unknown overlap of non-zero indices, and hence the size of the reduced result. We provide an adaptive set of techniques which can systematically handle all cases and their trade-offs. These algorithmic insights are backed by careful optimizations and additional system features.

Experimental Results. We validate SPARCML on a wide range of benchmarks: 1) synthetic instances aimed to validate our analysis, 2) academic benchmark datasets and models, and 3) an industrial-scale deployment for automated speech recognition (ASR), powering a popular personal assistant. Synthetic benchmarks show that SPARCML can bring order-of-magnitude speedups with respect to highly-optimized dense implementations, with limited overhead in the dense case. We incorporate SPARCML into two machine

learning frameworks: CNTK (developed by Microsoft) and MPI-OPT (developed by us). In the supercomputing deployment, SPARCML can reduce end-to-end convergence time of a state-of-the-art network for digit recognition by $3.65\times$, and completes a large-scale URL classification task $63\times$ faster than Spark MLlib [36]. On cloud-grade networks, SPARCML speeds up the same neural network training task by $19\times$, and completes the URL classification $86\times$ faster than Spark MLlib.

In the production deployment, SPARCML reduced the training time for a state-of-the-art ASR model on 128 GPUs by almost $10\times$ (from 14 days to 1.78 days), without significant accuracy loss. Our conclusion is that SPARCML regularly yields non-trivial speedups on a wide variety of machine learning applications, and that existing frameworks can still significantly speed up communication by leveraging sparsity and relaxed consistency guarantees.

2 Preliminaries

Notation. Throughout this paper, we use the following notation for input parameters:

Var	Description
P	Number of nodes
N	Problem dimension
p_i	Node i , $1 \leq i \leq P$
H_i	Set of non-zero indices which p_i wishes to communicate
k	Max number of non-zero (nnz) elements: $\max_i H_i $
\mathcal{K}	Total nnz in global sum: $ \cup_{i=1}^P H_i $
d	Density of non-zero elements: $\frac{k}{N}$

2.1 Data Parallelism

Data-parallelism is a classic distribution strategy for machine learning algorithms [1, 53]: nodes partition a large dataset and each maintains its own copy of the model. Model copies are kept in sync by frequently exchanging the model updates computed locally between nodes, either via global averaging of updates, or through a central coordinator [32]. In the context of the stochastic gradient descent (SGD) algorithm, each node has a dataset partition, and, in each *iteration*, it processes a randomly chosen set of samples (a *mini-batch*), and computes the model updates (gradients) locally using the classic SGD rule

$$\vec{x}_{t+1} = \vec{x}_t - \eta \nabla F(\vec{x}_t),$$

where \vec{x}_t is the value of the model at time t , η is the learning rate, and ∇F is the *stochastic* gradient of the current model with respect to the chosen set of samples.² Nodes average their gradient updates globally at the end of every iteration, so that they maintain a consistent version of the model. The trade-off in this setting is between the parallelism due to the fact that we are processing P times more samples per iteration given P nodes, and the additional communication cost due to maintaining a consistent model synchronously.

²For simplicity, the reader may think of the model \vec{x}_t as a large array of parameters, and of the gradient $\nabla F(\vec{x}_t)$ as an array of entry-wise updates.

Delayed Consistency. When distributing to large node counts, the above trade-off can shift towards synchronization cost, overwhelming the benefits of parallelism. Recent work [34,40], suggested that stochastic algorithms such as SGD can withstand a bounded amount of asynchrony, and still converge. The following condition, which we call *delayed consistency*, is sufficient:

Theorem 2.1 (Bounded Staleness [40], [34]). *SGD can still converge under asynchronous iterations, under standard assumptions, as long as there exists a uniform bound τ on the delay between the round at which an update is generated and the round at which the update is applied.*

Note that the value of τ can adversely impact the convergence rate of various algorithms [26, 34, 40]. Precisely characterizing these staleness-convergence-speed trade-offs is still a topic of active research and outside our scope.

Top- k SGD. Recent work proposes the following communication-reduced SGD variant called Top- k [2, 13]: each node communicates only the k largest (by magnitude) components of its gradient vector $\nabla F(\vec{x}_t)$, instead of all values in the traditional method. Usually, k is fixed to represent some percentage of the components, which can be $\leq 1\%$, which enforces high gradient sparsity at each node. This forces gradient sparsity at each node but the chosen components may vary across nodes. The other components are *accumulated*, and added to the gradient vector of the next iteration. Upon closer inspection, we notice that Top- k SGD can be seen as special case of *asynchronous* SGD, where the components which do not make the top- k at an iteration are *delayed* by being accumulated locally. This update model fits in the standard analyses of asynchronous SGD [40].

Stochastic Consistency. An orthogonal approach for reducing the communication cost of machine learning algorithms has been to *quantize* their updates, lowering the number of bits used to represent each value, e.g. [3, 12, 42, 50]. Such quantization techniques can also be shown to preserve correctness, as long as the quantization noise can be shown to be zero-mean [3]. We summarize this *stochastic consistency* condition as follows:

Theorem 2.2 (Stochastic Consistency [12], [3]). *SGD converges even under quantized noisy updates, under standard assumptions [3, 12], as long as the (noisy) gradient updates are unbiased, i.e., are corrupted with zero-mean noise.*

Relaxed Consistency in SPARCML. Our framework allows the user to leverage both delayed and stochastic consistency. In particular, we provide an efficient implementation of top- k SGD via sparse collective operations, with non-blocking semantics, as well as an implementation of state-of-the-art quantization methods [3].

2.2 Machine Learning Frameworks

MPI-OPT. MPI-OPT is a framework we developed to run distributed optimization algorithms such as SGD. It is written in native C++11, and can link external libraries such as SPARCML and MPI for communication. MPI-OPT implements parallel stochastic optimization algorithms, like gradient and coordinate descent, on multiple compute nodes communicating via any MPI library, with minimal overhead. It implements efficient distributed partitioning of any dataset converted in the predefined format using MPI-IO, data-parallel optimization on multiple compute nodes, with efficient multi-threading inside each node, parametrized learning rate adaptation strategies, as well as customizations to use SPARCML as the communication layer between nodes allowing for sparse, dense, synchronous, and asynchronous aggregation.

The Microsoft Cognitive Toolkit (CNTK). For large-scale neural network training, we modify CNTK [53] v2.0 to use SPARCML as its communication layer. We provide implementation details in Section 5. CNTK is a computational platform optimized for deep learning. The general principle behind CNTK is that neural network operations are described by a directed computation graph, in which leaf nodes represent input values or network parameters, and internal nodes represent matrix operations on their children. CNTK supports and implements most popular neural network architectures. To train such networks, CNTK implements stochastic gradient descent (SGD) with automatic differentiation. The CNTK baseline supports parallelization across multiple GPUs and servers, with efficient MPI-based communication.

3 Data Representation: Sparse Streams

We now describe the data types used to store sparse and dense vectors, which we call *sparse streams*. Sparse streams allow for efficient computation and communication of the data. Our implementation is in C++11, and we follow this standard in our description. For simplicity, we focus on the case where the binary operation executed upon two or multiple streams is *summation*, but the same discussion would apply for other component-wise operations.

Initially, we assume that each node is assigned a subset of non-zero elements from a universe of size N . Let H_i denote the set of non-zero elements given at node p_i . We assume that these sets are *sparse* with respect to N , i.e., that $k = \max_i |H_i| \ll N$. We further denote by d_i the density of each set given by $d_i = \frac{|H_i|}{N}$ and define $d = \max_i d_i = \frac{k}{N}$.

Define the total number of non-zero elements after having performed the reduction as

$$\mathcal{K} = |\cup_{i=1}^P H_i|.$$

For simplicity, we omit the very unlikely possibility of cancellation of indices during the summation and therefore get $k \leq \mathcal{K} \leq \min\{N, P \times k\}$.

Vector Representations. We start from a standard representation, storing a sparse vector as a sequence of non-zero indices, together with the actual scalar values of each dimension. (While more efficient but complex representations exist, they require additional computational effort.) The stream is stored in an array of consecutive index-value pairs. The datatype of the values yields the number of bits needed for every non-zero value. We either work with single (32 bits) or double precision floating point values (64 bits). We discuss lower precision support in Section 5. Given the dimension universe size N , we need at least $\lceil \log_2(N) \rceil$ bits for storing an index value.

Auto-Switching to a Dense Format. So far, the representation is straightforward. However, although we are interested in *sparse* problems, namely $k \ll N$, the size and non-zero index distribution of the input vectors can be such that the algorithm may not benefit from the sparse representation after some intermediate point in the summation process: if the density of the intermediate result vector reaches the universe size N , the sparse representation becomes wasteful.

We can model the benefits of sparsity as follows: Let *isize* be the number of bytes needed to represent a non-zero input value and *nnz* the number of non-zero elements. We further define $c \geq \lceil \frac{\log_2(N)}{8} \rceil$ to be the number of bytes needed to store an index. Thus, the sparse format will transmit $nnz(c + isize)$ bytes while

the dense format transmits $N \times \textit{isize}$ bytes. Our sparse representation only reduces the communication volume if $nnz \leq \delta = \frac{N \times \textit{isize}}{(c + \textit{isize})}$. Yet, this volume estimation does not capture the fact that summing sparse vectors is computationally more expensive than summing dense vectors. Thus, in practice, δ should be even smaller, to reflect this trade-off.

It is safe to assume that the initial $nnz = k$ is smaller than this threshold. However, as the summation advances and number of nonzero elements nnz in the vector grows, the condition $nnz \leq \delta$ may be violated. Especially for large node counts P , \mathcal{K} is almost certainly larger than δ . To address this dynamic fill-in, we add an extra value to the beginning of each vector that indicates whether the vector is dense or sparse. In fact, when allocating memory for vectors of dimension N , we request $N \times \textit{isize}$ bytes. It is therefore never possible to store more than δ sparse items. This threshold is used to automatically switch the representation.

Efficient Summation. The key operation is summing two vectors u_1 and u_2 , which could be either sparse or dense. To implement this operation efficiently, we first distinguish the case when u_1 and u_2 's indices come from any position between 1 and N , and can potentially overlap, from the case where the index sets are disjoint, which arises in instances where we partition the problem by dimension. This latter case is handled via concatenation.

If input indices can overlap, we distinguish the following cases, depending on whether inputs are sparse or dense. Denote by H_1 and H_2 the sets containing the sparse indices of non-neutral elements for the vectors u_1 and u_2 , respectively. If indices are overlapping, and both vectors are sparse, we first check whether the result might become dense. Theoretically, one needs to calculate the size of the union of non-zero indices $|H_1 \cup H_2|$. This is costly, and thus we only upper bound this result by $|H_1| + |H_2|$. (The tightness of this upper bound will depend on the underlying sparsity distribution, on which we make no prior assumptions.) If this value is bigger than δ , we switch to a dense representation. If one of the inputs is dense, whereas the other is sparse, we iterate over all the index-value pairs stored in the sparse vector and set the value at the corresponding position in the dense vector. Finally, if both vectors are already dense, we simply perform a (vectorized) dense vector summation in either u_1 or u_2 , and do not allocate a new stream.

4 Efficient Collectives on Sparse Streams

We now proceed to define collective operations over a set of sparse vectors located at different nodes. We focus on allgather and allreduce as defined by the MPI specification [16]. We support arbitrary coordinate-wise associative reduction operations for which a neutral-element can be defined. (By neutral element we mean an element which does not change the result of the underlying operation, e.g., 0 for the sum operation.) For simplicity, we outline the algorithms in terms of summation with the zero neutral element.

Analytical Model. We assume bidirectional, direct point-to-point communication between the nodes, and consider the classic Latency-Bandwidth (α - β) cost model: the cost of sending a message of size L is $T(L) = \alpha + \beta L$, where both α , the latency of a message transmission, and β , the transfer time per word, are constant. L represents the datum size in words or bytes. When sending sparse items, let β_s be the transfer time per sparse index-value pair. β_d represents the transfer time per value, and is smaller than β_s .

Given this setting, the goal is to perform a collective operation over the elements present initially at every node. That is, each node should obtain the correct result locally, i.e., the element-wise sum over the N

dimensions in the allreduce case, while minimizing the total communication costs, measured in the α - β model.

Assumptions. To facilitate the presentation, we will assume that each node initially has exactly k elements: $\forall i : |H_i| = k$; P is a power of 2, $P > 4$; and N is divisible by P . We give a thorough discussion of these assumptions and ways to relax them in the supplementary material.

4.1 Algorithms

Our main technical contribution consists of a set of algorithms to solve the sparse allreduce problem efficiently under various common input scenarios. An *allreduce* operation performs a global reduction operation on inputs located at *each node*, and distributes the result to *all nodes*. To implement allreduce, we utilize the *allgather* operation, an operation in which the data contributed by *each node* is gathered at *all nodes* (as opposed to a single root node). Both operations can be (inefficiently) implemented by performing a *Reduce* or *Gather* operation to a dedicated root, followed by a *Broadcast* to all the other nodes.

We emphasize that none of the following algorithms we propose requires knowledge about the amount of data contributed by each node, nor about the distribution of the non-zero indices. Nevertheless, depending on the size of the result \mathcal{K} , we will differentiate two types of instances: In *static sparse allreduce* (SSAR), \mathcal{K} remains below δ , such that we will never switch to a dense representation. Conversely, in *dynamic sparse allreduce* (DSAR) instances, where $\mathcal{K} \geq \delta$, we will start with a sparse and switch to a dense representation. We begin by discussing the most significant insights we gained to guide the reader through the section.

Generalization. Notice that the given definition of sparse allreduce with summation as its reduction operator is a generalization of both the well known allreduce and allgather collectives. The key distinction is that each node has some subset of non-zero (non-neutral) elements assigned initially. We can obtain instances of the classical problems as follows: First, if none of these non-zero index sets H_i overlap, we obtain an *allgather* instance on a subspace of N . Second, the *allreduce* problem is obtained if $H_i = H_j$ for all nodes i and j , that is, the sets fully overlap and therefore the reduced result has $|H_1|$ elements. If $|H_i| = N$ for all i , this is just dense allreduce. If $|H_i| = k < N$, we say that the problem is equivalent to a dense allreduce on a subspace of dimension k rather than N .

Based on this first simple insight, we can give an upper and lower bound on the runtime of every sparse allreduce algorithm. Performing an allgather operation, where each node contributes exactly k elements, results in a performance lower bound in this cost model of $\log_2(P)\alpha + (P - 1)k\beta_d$ [8].

The lower bound in terms of the α - β model for the allreduce collective with on vectors of size k is $\log_2(P)\alpha + 2\frac{P-1}{P}k\beta_d$, if we assume that the computational cost of the reduction is minimal [8]. Under this assumption, we obtain that:

Lemma 4.1. *Any algorithm solving the SSAR problem needs at least a duration of $\log_2(P)\alpha + (P - 1)k\beta_d$ if $\mathcal{K} = k \times P$, and $\log_2(P)\alpha + 2\frac{P-1}{P}k\beta_d$ assuming that $\mathcal{K} = k$ and computation for reduction is perfectly parallelized.*

We note that this lower bound is not tight in a setting where the computational cost is non-trivial. In that case, a simple pipelining algorithm on a ring topology will perform better, both in theory and in practice, e.g. [24]. We examine this algorithm in the experimental section.

Latency-Bandwidth Trade-Offs. A survey of algorithms for dense collectives including allreduce [24]

highlights the fact that single algorithms are not able to achieve both optimal latency and optimal bandwidth. Efficient MPI libraries such as MPICH or Open MPI therefore distinguish between small message sizes and long messages and switch between algorithms as appropriate [46]. We adopt a similar approach.

4.1.1 The Latency Dominated Case

When the overall reduced data is small, latency dominates the bandwidth term. In this case, we will adopt a *recursive doubling* technique: in the first round, nodes that are a distance 1 apart exchange their data and perform a local sparse stream reduction. In the second round, nodes that are a distance 2 apart exchange their reduced data. Following this pattern, in the t -th round, nodes that are a distance 2^{t-1} apart exchange all the previously reduced $2^{t-1}k$ data items. This behavior is illustrated in Figure 1. We use the same algorithm for solving a sparse allgather with non-overlapping indices and its more efficient summation in form of concatenation. The recursive doubling technique can also be used for solving *dense* allreduce and allgather problems [24].

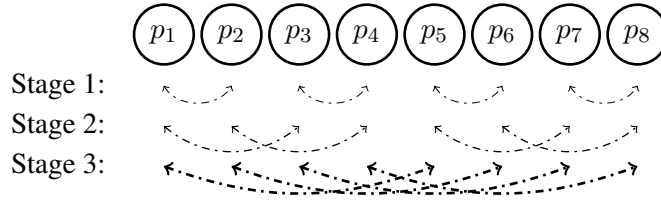


Figure 1: Static Sparse allreduce: Recursive doubling - Increasing amount of sparse data in every stage

The resulting latency for the `SSAR_Recursive_double` algorithm will be $L_1(P) = \log_2(P)\alpha$, as there are $\log_2(P)$ stages. This is optimal and data-independent. The runtime will lie in the range

$$L_1(P) + \log_2(P)k\beta_s \leq T_{ssar_rec_dbl} \leq L_1(P) + (P - 1)k\beta_s.$$

The lower bound is reached when the k indices fully overlap. Therefore, at every stage, k items need to be transmitted as the intermediate results maintain constant size. The upper bound is given when the indices do not overlap at all. Therefore, at stage t , the number of items transmitted is $2^{t-1}k$. Taking the sum, we get

$$\sum_{i=1}^{\log_2(P)} 2^{i-1}k = k \frac{2^{\log_2(P)} - 1}{2 - 1} = k(P - 1).$$

4.1.2 The Bandwidth Dominated Case

When the data is large, standard dense allreduce implementations make use of Rabenseifner’s algorithm [39], which has two steps. The first is a ReduceScatter step, which partitions the result vector across nodes, assigning a partition to each node. This is implemented by a *recursive halving* technique [39]. In the second step, the reduced answers are gathered to all other nodes by calling a recursive doubling algorithm as described above. This two step algorithm has a total runtime of

$$T_{ar_rab} = 2 \log_2(P)\alpha + 2 \frac{(P - 1)}{P} k\beta_s,$$

which reaches the lower bound on the bandwidth term and is off by a factor 2 on the latency term.

We will use a similar blueprint for Sparse allreduce, with some key differences. We split the algorithm into two steps: a *Split* phase and a *sparse allgather* phase. In the Split phase, we uniformly split the space dimension N into P partitions and assign to each node the indices contained in the corresponding partition. We split each sparse vector at its node and directly send each subrange of indices to the corresponding recipient in a *sparse* format. This direct communication comes at a theoretical price of higher latency cost, but by using non-blocking send and receive calls, the computation and communication can be nicely overlapped. Each node then reduces the data it received and builds the result for its partition. In the second phase, the data has to be gathered to all other nodes by using the previously described sparse allgather.

Obtaining runtime bounds for SSAR_Split_allgather is slightly more involved. The Split part takes time

$$(P - 1)\alpha + 0\beta_s \leq T_{split} \leq (P - 1)\alpha + k\beta_s.$$

Notice that both extremes imply that each node has k items for the sparse allgather and thus $\mathcal{K} = k \times P$ is reached. For this second step in the algorithm to be optimal, every node must have an intermediate result of size $\frac{k}{P}$, as we want the final result to have a size $\mathcal{K} = k$ and the communication to be equally distributed.

For every node to have an intermediate result of the desired size, we know that each node has to send at least $\frac{P-1}{P}k$ items to other nodes. Otherwise, if every node has exactly k items, we reach the upper bound for the result size of $\mathcal{K} = k \times P$. So we get

$$L_1(P) + \frac{P-1}{P}k\beta_s \leq T_{sparse.ag} \leq L_1(P) + (P-1)k\beta_s.$$

The algorithm latency is again data-independent:

$$L_2(P) = (P - 1)\alpha + L_1(P).$$

Combining these terms yields

$$L_2(P) + 2\frac{P-1}{P}k\beta_s \leq T_{ssar_split_ag} \leq L_2(P) + Pk\beta_s.$$

4.1.3 The Dynamic Case: Switching to Dense

The discussion so far focused on the case where maintaining a sparse representation is efficient. However, as we gather data, the size of the result \mathcal{K} might become larger than the sparsity-efficient threshold δ , in which case we switch to a dense representation. This is the *dynamic* version of the problem (DSAR). In this case, the following lower bound on the efficiency of the algorithm will hold.

Theorem 4.2. *Any algorithm solving the DSAR problem needs at least time $\log_2(P)\alpha + N\beta_d$.*

The proof follows directly on the latency term and directly holds on the bandwidth term from the fact, that each node has to receive or send at least $N - k$ items in order to become dense. From this observation we derive the following lemma, which says that, in this dynamic case, one can only hope to get a speedup of at most factor 2 compared to an optimal *dense* allreduce algorithm, focusing on the bandwidth term.

Lemma 4.3. *The bandwidth required by any algorithm for the DSAR problem is at least $\frac{1}{2}$ that of a bandwidth-optimal dense allreduce algorithm.*

Proof. Notice that the dense allreduce with $k = N$ has a lower bound of $2\frac{P-1}{P}N\beta_d$ on the bandwidth if computation is equally distributed. From Theorem 4.2 we know that every DSAR algorithm has a minimum bandwidth term of $N\beta_d$, which is obviously bigger than $\frac{P-1}{P}N\beta_d$ for any P . \square

Based on these insights, our solution for DSAR adapts the previous two-stage algorithm to exploit the fact that every reduced split will become dense. DSAR.Split.allgather hence receives the data in a sparse format from all the other nodes in the first phase, then switches the representation and performs a dense allgather in the second stage. Here, we can leverage existing implementations, which are highly optimized to perform this second step with dense data. Based on the known times needed by those algorithms, which are obviously input density independent, we derive the running time for our algorithm given both extremes. The latency is again $L_2(P)$. Combined, we get

$$L_2(P) + \frac{P-1}{P}N\beta_d \leq T_{dsar_split_ag}$$

and

$$T_{dsar_split_ag} \leq L_2(P) + k\beta_s + \frac{P-1}{P}N\beta_d.$$

Stochastic Analysis. In the additional material, we present an analysis of our algorithm in a stochastic setting, where the k non-zero indices at each processor are chosen randomly.

5 Artifact and Additional Features

Interface and Code. The SPARCML library provides an interface that is similar to that of standard MPI calls, with the caveat that the data representation is assumed to be a sparse stream. Given this, the changes needed to port MPI-enabled code to exploit sparsity through SPARCML are minor. The library implementation consists of around 2,000 lines of native C++11. (This does not include infrastructure such as benchmarks and tests which would raise the line count by an order of magnitude.) Adding SPARCML to CNTK required changing around 100 lines of code.

Non-Blocking Operations. We also implement the previous algorithms in a *non-blocking* way. Specifically, we allow a thread to trigger a collective operation, such as allreduce, in a nonblocking way. This enables the thread to proceed with local computations while the operation is performed in the background. For deep networks, we can nicely overlap communication and computation during the gradient aggregation phase by calling the aggregation per layer in a non-blocking fashion. As of MPI-3, implementations support non-blocking collective operations. However, rendering a custom operation implementation non-blocking is not entirely straightforward [22, 23] and needs to consider subtle message progression issues [21].

Low-Precision Support. To further reduce bandwidth cost, SPARCML supports lower-precision data representation for the updates, using QSGD quantization [3], which provably preserves the correctness of the algorithm. In brief, in this variant, each vector is split into *buckets* of size B (in the order of 1,024) and each bucket is quantized independently and stochastically. Thus, each bucket corresponds to B *low-precision data items*, e.g., 4-bit integers, packed to reduce space and a full-precision *scaling factor*. We focus on low-precision to reduce the bandwidth cost of the *dense* case. Hence, in the low-precision implementation, we either omit sparsity, or we use the low-precision data representation for the second part of the

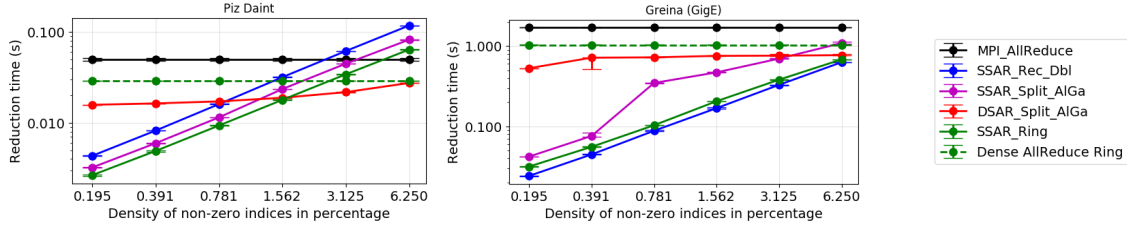


Figure 2: Data density versus reduction time for various algorithms, dimension $N = 16M$ and $P = 8$ nodes.

DSAR.Split.allgather algorithm, where the data becomes dense. Interestingly, by making use of this functionality, we are able to achieve speedup higher than $2\times$ compared to a fully dense allreduce, which was the upper bound when working with full-precision data.

6 Experiments

Setup. We now validate SPARCML on real world applications and synthetic experiments. Our experiments target two important scenarios: supercomputing and cloud computing. For the first setting, we execute on the CSCS Piz Daint supercomputer [7], with Cray XC50 nodes, each of which has a 12 cores HT-enabled Intel Xeon E5-2690 v3 CPU with 4GB RAM and an NVIDIA Tesla P100 16GB GPU. Piz Daint is currently the most powerful supercomputer in Europe (3rd in the world) and has a high-performance Cray Aries interconnect with a Dragonfly network topology. For the second setting, we use Amazon EC2 instances with a similar CPU configuration, but relatively older NVIDIA K80 GPUs, connected through Gigabit Ethernet. We perform additional tests on a cluster called Greina, with CX50 nodes and an InfiniBand FDR or Gigabit Ethernet interconnect and on a production-grade GPU cluster, described in the corresponding section.

In all our experiments, the baseline will be the MPI allreduce implementation on the fully dense vectors. On EC2, we make use of the default Open MPI installation optimized by Amazon. On Piz Daint, we compare against the custom Cray-MPICH installation, highly optimized by Cray. Since our problems usually have dimension $N > 65K$, we fix the datatype for storing an index to an `unsigned int`.

Name	# Classes	# of samples	Dimension
URL [35]	2	2 396 130	3 231 961
Webspam [49]	2	350 000	16 609 143
ImageNet [41]	1000	1,2 million	256x256x3
MNIST [31]	10	60 000	28x28
CIFAR-10 [29]	10	60 000	32x32x3
ATIS [18]	128	4 978 <i>s</i> / 56 590 <i>w</i>	-
Hansards [38]	-	948K <i>s</i> / 15 657K <i>w</i>	-

Table 1: Real World Application Datasets. *s* stands for sentences (or pairs) and *w* for words.

6.1 Micro-Benchmarks and Large-Scale Regression

We begin by validating our theoretical analysis on synthetic data, on the Piz Daint and Greina (GigE) clusters. We vary the data dimension N and the data density d as well as the number of nodes P . Based on the defined density, k indices out of N are selected uniformly at random at each node and are assigned a random value. We run our sparse allreduce algorithms in order to validate both correctness and the relative ordering of the derived analytical bounds. The choice of parameters to generate the data, is within reasonable ranges, seen in real world datasets. (E.g., we pick data dimensions corresponding to common layer sizes in neural networks.)

For readability, graphs are in a log-log scale. As execution times are non-deterministic, we conduct five experiments with newly generated data, while running each one for ten times. Based on those 50 resulting runtime values, we state the 25 and 75 percentage quantiles.

Following the theoretical analysis, we expect the variant `SSAR_Recursive_double` to perform best for a small amount of data, when latency dominates over the bandwidth term. At higher node count P , data becomes larger, which leads to less improvement of the algorithm `SSAR_Recursive_double` at the same number of non-zero entries over the other variants. Furthermore, the algorithm `SSAR_Split_allgather` dominates over the `DSAR_Split_allgather` variant as long as the number of non-zero indices is relatively low compared to the overall reduced size. To show the impact of the network on performance, we run identical tests on both Piz Daint and Greina (GigE) in Figure 2. The results confirm our analysis.

Additionally, the experiments in Figure 2 also compare our approaches against a ring-based MPI dense allreduce and its sparse counterpart. We note that, on a fast network and relatively small number of nodes, the ring-based algorithm is faster by a slight margin on the dense case, whereas the sparsity-based approach is more competitive on a relatively slower Gigabit Ethernet connection.

Large-Scale Regression. We use MPI-OPT to train linear classifiers (Logistic Regression, SVM) on large-scale classification datasets using SGD and SCD. The goal is to examine the runtime improvements by just exploiting the sparsity inherently present in the datasets and algorithms. The datasets are specified in Table 1. We make use of the binary classification datasets URL and Webspam.

For SGD, the samples (and hence, gradients) have high sparsity since the features are trigrams: while many such combinations exist, an item, e.g., a sentence, can only have a very limited set of them present. This is extremely common in text-based datasets. Since communication is lossless, convergence is preserved and we only report speedup of the communication and overall training time. We run SGD with large batches ($1,000 \times P$) for various combinations. The achieved speed of MPI-OPT with the best sparse reduction algorithm is reported in Table 2.

Additionally, we run SCD incorporated in MPI-OPT following the distributed implementation of [34]. We run the optimization on the logistic regression loss function for the URL dataset distributed on 8 nodes of Piz Daint to achieve identical convergence compared to SGD. Every node contributes 100 indices after every iteration. As the values calculated by each node lie in different slices of the entire model vector, we compare the runtime of a sparse allgather from SPARCML to its dense counterpart. MPI-OPT with a dense allgather has an average epoch time of 49 seconds, with 24 seconds dedicated to communication. The sparse allgather executes a dataset pass (epoch) in 26 seconds on average, with 4.5 seconds spent in the communication layer. This implies an overall speedup of factor $1.8\times$, due to a $5.3\times$ speedup in communication time.

Comparison with Apache Spark. Next, we compare MPI-OPT with Apache Spark v1.6, which is officially

System	Dataset	Model	# of nodes	Baseline Time (s)	Algorithm	Algo. Time (s)	Speedup
Piz Daint	Webspam	LR	32	2.40 (2.16)	SSAR_Recursive_double	0.68 (0.35)	3.53 (6.17)
		SVM	32	1.62 (1.42)		0.65 (0.44)	2.49 (3.23)
Piz Daint	URL	LR	32	2.64 (2.58)	SSAR_Recursive_double	0.75 (0.70)	3.52 (3.69)
		SVM	32	1.98 (1.93)		0.56 (0.53)	3.54 (3.64)
Piz Daint	Webspam	LR	8	4.67 (3.79)	SSAR_Split_allgather	2.56 (1.58)	1.82 (2.40)
	URL	LR	8	3.77 (3.53)		2.09 (1.50)	1.80 (2.35)
Greina (IB)	Webspam	LR	8	6.52 (4.67)	SSAR_Split_allgather	3.63 (1.90)	1.80 (2.46)
	URL	LR	8	8.14 (4.47)		6.11 (2.49)	1.33 (1.80)
Greina (GigE)	Webspam	LR	8	76.80 (75.95)	SSAR_Split_allgather	3.79 (2.95)	20.26 (25.75)
	URL	LR	8	104.50 (100.46)		8.26 (4.22)	12.65 (23.81)

Table 2: Distributed optimization using MPI-OPT. The times are averages for a full dataset pass, with the communication part in brackets. Speedup versus dense MPI is shown end-to-end, with communication speedup in brackets.

supported by CSCS [6]. Comparison is performed on the same datasets, with the note that Spark uses its own communication layer and does not exploit sparsity. On the Piz Daint supercomputer, using 8 nodes, MPI-OPT with SPARCML reduces the time to convergence on the URL dataset by $63\times$. This is largely due to the reduction in communication time, which we measure to be of $185\times$. Concretely, the average epoch time is reduced from 378 seconds, with 319 seconds spent for communication, to an average of 6 seconds per epoch, whereof 1.7 seconds represent the communication time. Compared to Spark, MPI-OPT with the standard Cray-optimized *dense* allreduce has a $31\times$ speedup to convergence, due to a $43\times$ speedup in communication time. An epoch is executed in 13 seconds on average, with 8.6 seconds spent on communication. We further investigated these speedups on an 8-node research cluster with a Gigabit Ethernet interconnection. This mimics an Amazon EC2 scenario, with no background traffic. Using MPI-OPT, the average training time per epoch drops from 1,274 seconds (Spark) to 14 seconds, representing a speedup of $86\times$. On the communication part, the time per epoch drops from 1,042 seconds to 6 seconds. The communication time and overall speedup of a *dense* allreduce over Spark’s communication layer are both of factor $12\times$.

6.2 Training Deep Neural Networks

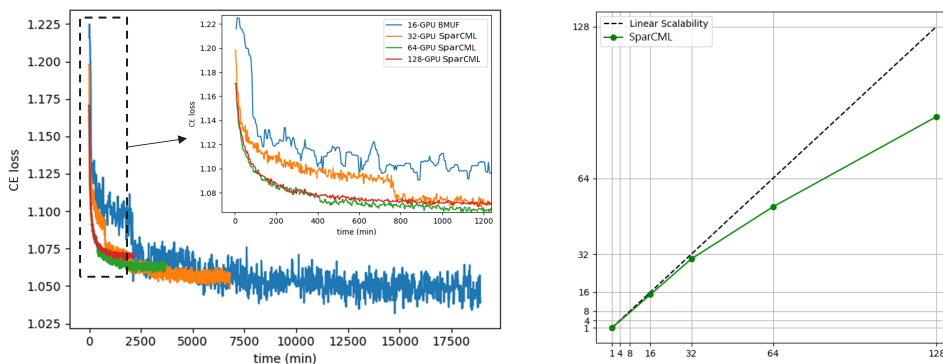
Next, we turn to training state-of-the-art deep neural networks in CNTK, using SPARCML. To exploit sparsity, we use the Top- k SGD algorithm [2, 13, 44], combined with low-precision support [3]. We execute three types of tasks: *image classification* on the ImageNet, CIFAR-10, and MNIST datasets, *natural language understanding* on the ATIS corpus and *machine translation* on the Hansards dataset. The datasets are specified in Table 1. For vision, we run experiments on the following deep networks: AlexNet [30], VGG [43], ResNet [17] and multi layer perceptrons (MLPs) with fixed numbers, two hidden layers of dimension 4,096 each. For natural language understanding and machine translation we use an encoder-decoder network consisting of two LSTM [20] cells each.

For this, we have interfaced SPARCML into CNTK. We make use of the non-blocking version of the sparse allreduce algorithm when working with full precision. Selecting the biggest elements in magnitude is implemented efficiently in CNTK by building “buckets” with 512 consecutive tensor elements each (reshaping

the tensor when necessary), and implementing a fast randomized Top- k algorithm. This enables fast computation on GPUs and allows for significant speedup over the fully dense allreduce variant. We use standard batch sizes and default hyper-parameters for 32-bit full accuracy convergence in all our experiments. These values are given in the open-source CNTK 2.0 repository. We have also experimented with supporting the 1-bit SGD quantization algorithm [42] and asynchronous (ASGD) training. Unfortunately, for 1-bit SGD, the way tensors in convolutional layers are handled, can actually *increase* overall training time with respect to the MPI baseline in networks with lots of convolutions, such as ResNet. ASGD training requires extremely careful hyperparameter tuning to maintain accuracy [54] and is therefore left for future work.

Accuracy & Speedup. As stated by in the preliminaries, working with delayed consistency might affect convergence speed, as the sparsity-accuracy trade-offs are not yet fully understood. Similarly to [2, 13], experiments on MNIST with multi-layer perceptrons (MLPs), CIFAR-10 on ResNet110 and ATIS with LSTMs show almost identical convergence speed even when forcing high sparsity. When combining Top- k and quantization with selecting $k = 16$ out of every bucket of size 512 and quantizing the dense values using 4-bit precision we achieve a top-1 accuracy 0.48% below the full precision and even increase top-5 accuracy by 0.12% on the CIFAR-10 dataset. For MNIST, the training error fluctuates by less than 0.1%. Comparing the overall epoch time on this last task to a full dense reduction implementation reveals its impact of system choice. We achieve a overall speedup of factor $19.12\times$ on a 8 node Amazon EC2 cluster with Gigabit Ethernet interconnection, whereas the speedup factor on the high performance network on Piz Daint reaches a factor $3.65\times$. We furthermore conduct neural machine translation experiments on the Hansards dataset using an encoder-decoder network with two LSTM cells each. By selecting the 4 largest values out of each 512 consecutive elements, we achieve an overall speedup of factor $1.54\times$ with slightly worse convergence speed on 8 nodes of Piz Daint.

We have also applied Top- k SGD on the ImageNet dataset, but found that reaching full accuracy requires significant additional hyper-parameter tuning. Recent work reports accurate training at extremely high sparsity levels on this dataset [33], but we were not able to successfully replicate these results on our setup within our computational budget.



(a) Numbers are for 6 training passes over the entire dataset, recording training error (CE loss). Validation results (word-error-rates) are discussed in the text.

(b) SparCML Scalability

Figure 3: Production Workload Speech Experiments.

6.3 Production Workload Experiments

The final test of our framework is on a state-of-the-art acoustic model for automated speech recognition (ASR), powering a popular digital personal assistant. The model we train is a state-of-the-art LSTM network with attention. The model has more than 60 million parameters, 2.4 million of which reside in the attention layer. We employ Top- k SGD for the training of the attention layer, starting from a pre-trained LSTM network. The dataset consists of approximately 30,000 hours (3.5 years) of annotated speech. Our cluster deployment consists of 32 server nodes, each with four NVIDIA V100 GPUs, totalling 128 GPUs. Aggregation inside each node is performed via NVIDIA NCCL [37].

The baseline we compare against is training on 4 nodes, 16 GPUs in total, without sparsity or quantization, but employing a carefully-tuned instance of block-momentum SGD (BMUF) [9]. Higher node counts for this variant lead to negative scalability and, in some cases, divergence. We note that this baseline already performs non-trivial communication reduction, since it communicates updates less frequently between nodes with respect to standard minibatch SGD. (Standard minibatch SGD is infeasible on our setup due to the large model size and node count.)

We execute the standard training protocol for this model: six training passes over the entire dataset, registering the time to complete the experiment and the training accuracy, after which we perform validation on a series of proprietary datasets which have not been used during training. In this second stage, we record word-error-rates (WER) for the model. The 16 GPU BMUF baseline takes approximately 14 days to complete training. We compare against our version of Top- k SGD with SPARCML, in which gradients are split into groups of 512 consecutive coordinates, out of which we select the 4 largest ones, which we transmit from each group, saving the rest locally. This corresponds to $< 0.8\%$ density of the gradient updates. We aim to leverage the fact that, in this production setting, most updates will occur in the parameters of the attention layer.

Figure 3a presents the results in training-error-versus-time format, where error is measured by standard cross-entropy (CE) loss, using our implementation, for 32, 64, and 128 GPUs. We highlight the fact that the sparse implementation is able to reach similar accuracy in a fraction of the time: at 128 GPUs, we are able to reduce training time to < 1.8 days. Figure 3b highlights the good scalability of the method. We closely examined the test error in terms of word-error-rate (WER) for the converged models, on validation sets. We found that the models trained with SparCML incur error rates that usually *on par* with the full-precision baseline: errors are less than 1% higher than full-precision (but unscalable) training and sparse training can *improve* accuracy by up to 1% on some validation datasets. This trade-off is very advantageous for our application scenario.

7 Related Work

There has been a surge of interest in distributed machine learning; see Ben-Nun and Hoefler [5] for a survey. We will focus on references that are closely related to our work.

Reduced Communication Techniques. Seide et al. [42] was among the first to propose quantization to reduce the bandwidth and latency costs of training deep networks. More recently, Alistarh et al. [3] introduced a theoretically-justified distributed SGD variant called Quantized SGD (QSGD), which allows the user to trade off compression and convergence rate. We implement QSGD as a default quantization method.

Dryden et al. [13] and Aji and Heafield [2] considered an alternative approach to communication reduction for data-parallel SGD, *sparsifying* the gradient updates by only applying the top- k components, taken at every node, in every iteration, for k corresponding to $< 1\%$ of the update size. Since then, other references [33, 44] explored this space, showing that extremely high gradient sparsity ($< 0.1\%$) can be supported by convolutional and recurrent networks with preserved accuracy, although maintaining accuracy requires very careful tuning of hyperparameters.

We complement this work by providing efficient sparsity support, with consistent runtime gains in large-scale settings.

Lossless Methods. One loss-less communication-reduction technique is *factorization* [11, 51], effective in deep neural networks with large fully-connected layers. This is less applicable in networks with large convolutional layers, which is the case for many modern architectures [17, 45]. Poseidon / Petuum [51] is a complete distributed machine learning framework built on the idea of reducing communication through factorization. A second such method is executing *extremely large batches*, thus hiding the cost of communication behind larger computation [15, 52]. Although promising, large-batch methods require careful per-instance parameter tuning and do not eliminate communication costs.

Communication Frameworks. Several frameworks have been proposed for reducing communication cost of distributed machine learning. One popular example is NVIDIA’s NCCL framework [37], which significantly reduces communication cost when the nodes are NVIDIA GPUs and the proprietary NVLINK interconnect is available, which is not the case in multi-node settings, such as supercomputing. Further, NCCL currently only implements a very restricted set of reduction operations. In addition, there is a non-trivial number of frameworks customized to specific application scenarios, such as the Livermore Big Artificial Neural Network Toolkit (LBANN) [48] or S-Caffe [4]. While very efficient in specific instances, these frameworks do not usually leverage reduced-communication techniques, or sparsity.

Sparse Reduction. Efficient MPI support for reductions over sparse input vectors was considered by [25] and from the algorithmic perspective in [47]. The first reference proposes and evaluates a direct runlength encoding approach; we significantly extend this approach in the current work, including the observation that data might become dense during the reduction process and that an efficient and flexible data representation must be provided in this case. Kylix [55] considers sparse many-to-many reductions in the context of computation over large scale distributed graph data on community clusters. However, Kylix assumes knowledge of the data distribution and performs multiple passes over the reduction, which make it not applicable to our scenario. Dryden et al. [13] implement a sparse variant of the classical allreduce algorithm via a pairwise reduce-scatter followed by a ring-based allgather. The amount of data is kept constant at every stage of their algorithm by re-selecting the top k values and postponing the other received values. We note that this ability to preserve a local residual is specific to Top- k SGD and that our framework is more general. In terms of performance, their implementation will provide similar results to our SSAR_Split_allgather implementation.

8 Conclusions and Further Work

We have described and analyzed SPARCML, a high-performance communication framework that allows the user to leverage sparse and low-precision communication in the context of machine learning algorithms.

Due to its compatibility with MPI semantics, SPARCML integrates easily into existing computational frameworks and can provide order-of-magnitude speedups in several real-world applications.

We aim to further investigate other distributed machine learning algorithms which can benefit from sparsity, such as distributed principal component analysis (PCA) and k-means clustering (Lloyd’s algorithm). We believe that the simple but effective sparsity schemes we described can play a significant role in reducing communication cost in future distributed machine learning systems.

References

- [1] ABADI, M., BARHAM, P., CHEN, J., CHEN, Z., DAVIS, A., DEAN, J., DEVIN, M., GHEMAWAT, S., IRVING, G., ISARD, M., ET AL. Tensorflow: A system for large-scale machine learning. In *OSDI* (2016), vol. 16, pp. 265–283.
- [2] AJI, A. F., AND HEAFIELD, K. Sparse communication for distributed gradient descent. *arXiv preprint arXiv:1704.05021* (2017).
- [3] ALISTARH, D., GRUBIC, D., LI, J., TOMIOKA, R., AND VOJNOVIC, M. QSGD: Randomized quantization for communication-efficient stochastic gradient descent. In *Proceedings of NIPS 2017* (2017).
- [4] AWAN, A. A., HAMIDOUCHE, K., HASHMI, J. M., AND PANDA, D. K. S-caffe: Co-designing mpi runtimes and caffe for scalable deep learning on modern gpu clusters. In *Proceedings of the 22nd ACM SIGPLAN Symposium on Principles and Practice of Parallel Programming* (2017), ACM, pp. 193–205.
- [5] BEN-NUN, T., AND HOEFLER, T. Demystifying Parallel and Distributed Deep Learning: An In-Depth Concurrency Analysis. *CoRR abs/1802.09941* (Feb. 2018).
- [6] CENTRE, C. S. N. S. Apache Spark on the CSCS Cluster. https://user.cscs.ch/scientific_computing/supported_applications/spark/, August 2018.
- [7] CENTRE, C. S. N. S. The CSCS Piz Daint supercomputer. http://www.cscs.ch/computers/piz_daint, August 2018.
- [8] CHAN, E., HEIMLICH, M., PURKAYASTHA, A., AND VAN DE GEIJN, R. Collective communication: theory, practice, and experience. *Concurrency and Computation: Practice and Experience* 19, 13 (2007), 1749–1783.
- [9] CHEN, K., AND HUO, Q. Scalable training of deep learning machines by incremental block training with intra-block parallel optimization and blockwise model-update filtering. In *Acoustics, Speech and Signal Processing (ICASSP), 2016 IEEE International Conference on* (2016), IEEE, pp. 5880–5884.
- [10] CHEN, T., LI, M., LI, Y., LIN, M., WANG, N., WANG, M., XIAO, T., XU, B., ZHANG, C., AND ZHANG, Z. Mxnet: A flexible and efficient machine learning library for heterogeneous distributed systems. *arXiv preprint arXiv:1512.01274* (2015).
- [11] CHILIMBI, T. M., SUZUE, Y., APACIBLE, J., AND KALYANARAMAN, K. Project adam: Building an efficient and scalable deep learning training system. In *OSDI* (2014), vol. 14, pp. 571–582.

- [12] DE SA, C., ZHANG, C., OLUKOTUN, K., AND RÉ, C. Taming the wild: A unified analysis of Hogwild. *Style Algorithms. In NIPS* (2015).
- [13] DRYDEN, N., JACOBS, S. A., MOON, T., AND VAN ESSEN, B. Communication quantization for data-parallel training of deep neural networks. In *Proceedings of the Workshop on Machine Learning in High Performance Computing Environments* (2016), IEEE Press, pp. 1–8.
- [14] FORUM, M. P. I. MPI: A Message-Passing Interface Standard Version 3.0, 09 2012.
- [15] GOYAL, P., DOLLÁR, P., GIRSHICK, R., NOORDHUIS, P., WESOŁOWSKI, L., KYROLA, A., TULLOCH, A., JIA, Y., AND HE, K. Accurate, large minibatch sgd: Training imagenet in 1 hour. *arXiv preprint arXiv:1706.02677* (2017).
- [16] GROPP, W., HOEFLER, T., THAKUR, R., AND LUSK, E. *Using Advanced MPI: Modern Features of the Message-Passing Interface*. MIT Press, Nov. 2014.
- [17] HE, K., ZHANG, X., REN, S., AND SUN, J. Deep residual learning for image recognition. In *Proceedings of the IEEE conference on computer vision and pattern recognition* (2016), pp. 770–778.
- [18] HEMPHILL, C. T., GODFREY, J. J., DODDINGTON, G. R., ET AL. The atis spoken language systems pilot corpus. In *Proceedings of the DARPA speech and natural language workshop* (1990), pp. 96–101.
- [19] HENSGEN, D., FINKEL, R., AND MANBER, U. Two algorithms for barrier synchronization. *International Journal of Parallel Programming* 17, 1 (1988), 1–17.
- [20] HOCHREITER, S., AND SCHMIDHUBER, J. Long short-term memory. *Neural computation* 9, 8 (1997), 1735–1780.
- [21] HOEFLER, T., AND LUMSDAINE, A. Message Progression in Parallel Computing - To Thread or not to Thread? In *Proceedings of the 2008 IEEE International Conference on Cluster Computing* (Oct. 2008), IEEE Computer Society.
- [22] HOEFLER, T., LUMSDAINE, A., AND REHM, W. Implementation and performance analysis of non-blocking collective operations for mpi. In *Supercomputing, 2007. SC'07. Proceedings of the 2007 ACM/IEEE Conference on* (2007), IEEE, pp. 1–10.
- [23] HOEFLER, T., LUMSDAINE, A., AND REHM, W. Implementation and Performance Analysis of Non-Blocking Collective Operations for MPI. In *Proceedings of the 2007 International Conference on High Performance Computing, Networking, Storage and Analysis, SC07* (Nov. 2007), IEEE Computer Society/ACM.
- [24] HOEFLER, T., AND MOOR, D. Energy, Memory, and Runtime Tradeoffs for Implementing Collective Communication Operations. *Journal of Supercomputing Frontiers and Innovations* 1, 2 (Oct. 2014), 58–75.
- [25] HOFMANN, M., AND RÜNGER, G. Mpi reduction operations for sparse floating-point data. *Lecture Notes in Computer Science* 5205 (2008), 94.
- [26] JIANG, J., CUI, B., ZHANG, C., AND YU, L. Heterogeneity-aware distributed parameter servers. In *Proceedings of the 2017 ACM International Conference on Management of Data* (New York, NY, USA, 2017), SIGMOD '17, ACM, pp. 463–478.

- [27] JOUPPI, N. P., YOUNG, C., PATIL, N., PATTERSON, D., AGRAWAL, G., BAJWA, R., BATES, S., BHATIA, S., BODEN, N., BORCHERS, A., ET AL. In-datacenter performance analysis of a tensor processing unit. *arXiv preprint arXiv:1704.04760* (2017).
- [28] KETKAR, N. Introduction to pytorch. In *Deep Learning with Python*. Springer, 2017, pp. 195–208.
- [29] KRIZHEVSKY, A., AND HINTON, G. Learning multiple layers of features from tiny images.
- [30] KRIZHEVSKY, A., SUTSKEVER, I., AND HINTON, G. E. Imagenet classification with deep convolutional neural networks. In *Advances in neural information processing systems* (2012), pp. 1097–1105.
- [31] LECUN, Y., AND CORTES, C. MNIST handwritten digit database.
- [32] LI, M., ANDERSEN, D. G., PARK, J. W., SMOLA, A. J., AHMED, A., JOSIFOVSKI, V., LONG, J., SHEKITA, E. J., AND SU, B.-Y. Scaling distributed machine learning with the parameter server. In *OSDI* (2014), vol. 1, p. 3.
- [33] LIN, Y., HAN, S., MAO, H., WANG, Y., AND DALLY, W. J. Deep gradient compression: Reducing the communication bandwidth for distributed training. *arXiv preprint arXiv:1712.01887* (2017).
- [34] LIU, J., AND WRIGHT, S. J. Asynchronous stochastic coordinate descent: Parallelism and convergence properties. *SIAM Journal on Optimization* 25, 1 (2015), 351–376.
- [35] MA, J., SAUL, L. K., SAVAGE, S., AND VOELKER, G. M. Identifying suspicious urls: an application of large-scale online learning. In *Proceedings of the 26th annual international conference on machine learning* (2009), ACM, pp. 681–688.
- [36] MENG, X., BRADLEY, J., YAVUZ, B., SPARKS, E., VENKATARAMAN, S., LIU, D., FREEMAN, J., TSAI, D., AMDE, M., OWEN, S., ET AL. Mllib: Machine learning in apache spark. *The Journal of Machine Learning Research* 17, 1 (2016), 1235–1241.
- [37] NVIDIA. The nvidia collective communications library (nccl). <https://developer.nvidia.com/nccl> (2016).
- [38] OF THE USC INFORMATION SCIENCES INSTITUTE, N. L. G. Aligned Hansards of the 36th Parliament of Canada, October 2017.
- [39] RABENSEIFNER, R. Optimization of collective reduction operations. In *International Conference on Computational Science* (2004), Springer, pp. 1–9.
- [40] RECHT, B., RE, C., WRIGHT, S., AND NIU, F. Hogwild: A lock-free approach to parallelizing stochastic gradient descent. In *Advances in neural information processing systems* (2011), pp. 693–701.
- [41] RUSSAKOVSKY, O., DENG, J., SU, H., KRAUSE, J., SATHEESH, S., MA, S., HUANG, Z., KARPATHY, A., KHOSLA, A., BERNSTEIN, M., ET AL. Imagenet large scale visual recognition challenge. *International Journal of Computer Vision* 115, 3 (2015), 211–252.
- [42] SEIDE, F., FU, H., DROPPA, J., LI, G., AND YU, D. 1-bit Stochastic Gradient Descent and its Application to Data-parallel Distributed Training of Speech DNNs. In *Fifteenth Annual Conference of the International Speech Communication Association* (2014).

- [43] SIMONYAN, K., AND ZISSERMAN, A. Very deep convolutional networks for large-scale image recognition. *arXiv preprint arXiv:1409.1556* (2014).
- [44] SUN, X., REN, X., MA, S., AND WANG, H. meprop: Sparsified back propagation for accelerated deep learning with reduced overfitting. *arXiv preprint arXiv:1706.06197* (2017).
- [45] SZEGEDY, C., IOFFE, S., VANHOUCHE, V., AND ALEMI, A. A. Inception-v4, inception-resnet and the impact of residual connections on learning. In *AAAI* (2017), pp. 4278–4284.
- [46] THAKUR, R., AND GROPP, W. D. Improving the performance of collective operations in mpich. In *European Parallel Virtual Machine/Message Passing Interface Users Group Meeting* (2003), Springer, pp. 257–267.
- [47] TRÄFF, J. Transparent neutral element elimination in mpi reduction operations. *Recent Advances in the Message Passing Interface* (2010), 275–284.
- [48] VAN ESSEN, B., KIM, H., PEARCE, R., BOAKYE, K., AND CHEN, B. Lbann: Livermore big artificial neural network hpc toolkit. In *Proceedings of the Workshop on Machine Learning in High-Performance Computing Environments* (2015), ACM, p. 5.
- [49] WEBB, S., CAVERLEE, J., AND PU, C. Introducing the webb spam corpus: Using email spam to identify web spam automatically. In *CEAS* (2006).
- [50] WEN, W., XU, C., YAN, F., WU, C., WANG, Y., CHEN, Y., AND LI, H. Terngrad: Ternary gradients to reduce communication in distributed deep learning. In *Advances in Neural Information Processing Systems* (2017), pp. 1508–1518.
- [51] XING, E. P., HO, Q., DAI, W., KIM, J. K., WEI, J., LEE, S., ZHENG, X., XIE, P., KUMAR, A., AND YU, Y. Petuum: A new platform for distributed machine learning on big data. *IEEE Transactions on Big Data* 1, 2 (2015), 49–67.
- [52] YOU, Y., GITMAN, I., AND GINSBURG, B. Scaling sgd batch size to 32k for imagenet training. *arXiv preprint arXiv:1708.03888* (2017).
- [53] YU, D., EVERSOLE, A., SELTZER, M., YAO, K., HUANG, Z., GUENTER, B., KUCHAIEV, O., ZHANG, Y., SEIDE, F., WANG, H., ET AL. An introduction to computational networks and the computational network toolkit. *Microsoft Technical Report MSR-TR-2014-112* (2014).
- [54] ZHANG, J., MITLIAGKAS, I., AND RÉ, C. Yellowfin and the art of momentum tuning. *arXiv preprint arXiv:1706.03471* (2017).
- [55] ZHAO, H., AND CANNY, J. Kylix: A sparse allreduce for commodity clusters. In *Parallel Processing (ICPP), 2014 43rd International Conference on* (2014), IEEE, pp. 273–282.

A Relaxation of Assumption in Section 4

Even though the three assumptions given in Section 4 simplify the formulas in the subsequent analysis of the algorithms, they do not oversimplify the problem. Ignoring assumption (1) and having $k = \max_i |H_i|$, one gets an upper bound on each algorithm. This upper bound only makes sense if we assume approximately an equal number of non-zero elements at every node. Otherwise, one could imagine to design more specific algorithms. If assumption (2) does not hold, one can add two additional steps in front and at the end of every algorithm to reduce the number of participating nodes to the nearest lower power of two. Although this might not be optimal (a dissemination approach [19] might be favorable), the cost increases by some constant value and thus, we still get an idea about which algorithm to prefer. If assumption (3) does not hold, each node gets responsible of $\lfloor \frac{N}{P} \rfloor$ items apart of the last one, which is responsible of $N - (P - 1)\lfloor \frac{N}{P} \rfloor$ items.

B Stochastic Analysis

We realize, the difficulty of designing any efficient algorithms comes from the fact that we neither know in advance the exact number of items every node contributes, nor the size any intermediate, or the final result will have. This data has to be communicated across the network. Those result sizes are not only dependent on the amount of data contributed by each node, but also alters with different positions of the non-neutral indices. If one assumes an underlying probability distribution of the non-zero elements, one can define the expected total number of non-zero elements $\mathbb{E}[\mathcal{K}]$. We therefore make use of N Bernoulli random variables $X_j = 1$, if index $j \in \cup_{i=1}^P H_i$, and $X_j = 0$ otherwise, for $1 \leq j \leq N$. The random variable $Y = \sum_{j=1}^N X_j$ then represents the total number of non-zero entries after having performed the reduction. By using the linearity property of the expectation, we get:

$$\mathbb{E}[\mathcal{K}] = \mathbb{E}[Y] = \sum_{j=1}^N P(j \in \cup_{i=1}^P H_i).$$

The probability of any index j being an element of a distinct set H_i is given by the underlying distribution. It is true for any distribution that:

$$P(j \in \cup_{i=1}^P H_i) = \sum_{i=1}^P P(j \in H_i) - \sum_{i < k} P(j \in (H_i \cap H_k)) + \sum_{i < k < l} P(j \in (H_i \cap H_k \cap H_l)) \dots + (-1)^{P-1} P(j \in \cap_{i=1}^P H_i).$$

We further know from Union Bound that $P(j \in \cup_{i=1}^P H_i) \leq \sum_{i=1}^P P(j \in H_i)$, which gives us a valuable upper bound on the expected number of non-zero elements

$$\mathbb{E}[Y] \leq \sum_{j=1}^N \sum_{i=1}^P P(j \in H_i).$$

This bound is tight if $\forall i < j : H_i \cap H_j = \emptyset$, which is the special case where the problem reduces to an allgather.

B.1 Uniform Distribution

Having derived those formulas, we give more concrete values by assuming a uniform distribution. This use-case gives a worst-case scenario in terms of probabilistic growth of the intermediate results and it is reasonable to make this assumption, if every index is hit with probability higher than 0. For this, let H_i consist of k independent samples drawn from a uniform distribution

$$j \sim \mathcal{U}(1, N) \quad \forall j \in H_i,$$

therefore $P(j \in H_i) = \frac{k}{N}$. This is independent of the two indices i and j in the above general formula, so $\mathbb{E}[\mathcal{K}] \leq N \times P \times \frac{k}{N} = P \times k$, which fits the non-probabilistic upper bound given earlier. For the uniform distribution one can give the exact expected number of elements by deriving a closed-form function utilizing the previous equations

$$\mathbb{E}[\mathcal{K}] = f(k, N, P) = N \times \left(\sum_{i=1}^P (-1)^{i-1} \binom{P}{i} \left(\frac{k}{N} \right)^i \right).$$

Figure 4 illustrates the multiplicative growth dependent on both inputs, the number of nodes P and the number of non-zero entries k at each node.

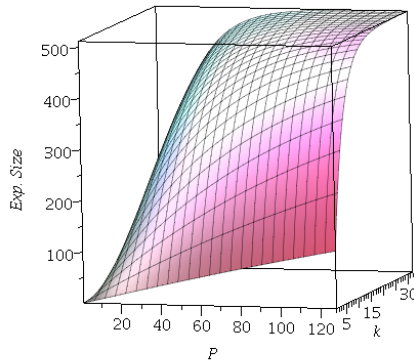


Figure 4: Expected size of reduced result assuming a uniform distribution and $N = 512$